Angle-resolved photoemission studies of Ge(111)-$c(2\times8)$, Ge(111)-(1×1)H, Si(111)-(7×7), and Si(100)-(2×1)

A. L. Wachs, T. Miller, T. C. Hsieh, A. P. Shapiro, and T.-C. Chiang
Department of Physics and Materials Research Laboratory, University of Illinois at Urbana—Champaign, Urbana, Illinois 61801
(Received 26 February 1985)

Angle-resolved photoemission measurements have been carried out for Ge(111)-$c(2\times8)$, Ge(111)-(1×1)H, Si(111)-(7×7), and Si(100)-(2×1) in a normal emission geometry over a wide photon energy range. For Ge(111) and Si(100), dispersive bulk-derived transitions were observed, from which we have determined the bulk valence-band dispersion relations for Ge along the [111] direction and for Si along the [100] direction in the Brillouin zone. The results are compared with the theoretical band dispersions of Chelikowsky and Cohen [Phys. Rev. B **14**, 556 (1976)]. For Si(111)-(7×7), the spectra are dominated by nondispersive features which cannot be used for band mapping. The lack of dispersive bulk-transition features for Si(111)-(7×7) is explained in terms of a relatively extended near-surface strain field which renders the electron crystal momentum highly mixed. Several surface-state features on these surfaces were also observed; most of them are visible over a very wide photon energy range and are indeed dispersionless, confirming the previous surface-state assignments.

I. INTRODUCTION

There have been a number of photoemission studies in recent years of the electronic properties of group-IV semiconductors. Many surfaces, including Ge(111)-$c(2\times8)$, Ge(111)-(2×1), Si(111)-(2×1), Si(111)-(7×7), Si(100)-(2×1), Ge(100)-(2×1), etc. have been examined.[1–14] On many of these surfaces, surface electronic states have been observed and their band dispersions have been determined. The theoretical and experimental properties of these surfaces have been reviewed.[1,2]

The bulk valence-band structures of germanium and silicon are likely to be the most studied of all semiconductors.[15] Chelikowsky and Cohen[16] have obtained a theoretical picture of Si and Ge band structure by combining x-ray photoelectron spectroscopy and optical measurements with an empirical nonlocal pseudopotential calculation. There are few direct experimental band mapping measurements however, and only very limited parts of the bulk band dispersions have been directly determined from experiment. For example, two angle-resolved photoemission studies have been performed to determine the upper bulk valence-band dispersions along the $\langle 100\rangle$ direction of Ge.[11,12] In comparison, the bulk valence-band dispersion relations of GaAs have been determined experimentally over a much wider range of k space.[17,18] A recent k-resolved inverse photoemission study mapped out the dispersion of the two lowest conduction bands in silicon and determined the energies of the L_1^c and L_3^c critical points.[19]

In this paper, we present angle-resolved photoemission studies of Ge(111)-$c(2\times8)$, Si(111)-(7×7), and Si(100)-(2×1) over a wide photon energy range. The data samples a wide range of k space. Using a free-electron approximation for the final-state dispersions,[17,18] which has proved to be an excellent approximation in the case of GaAs, we have determined bulk valence-band dispersions for Ge from the Γ point to the L point along the [111] direction of the Brillouin zone; the results are in excellent agreement with theory.[16] We have also determined part of the bulk Si valence-band dispersions along the [100] direction of the Brillouin zone. We were unable to obtain bulk valence-band dispersions from the Si(111)-(7×7) data. We discuss the implications of this result with regard to near-surface strain of Si(111)-(7×7).

The Si(100)-(2×1), Si(111)-(7×7), and Ge(111)-$c(2\times8)$ data also contain surface-state spectral features, which have been observed and identified by other authors.[1–14] The identification of surface-state spectral features in many of the previous publications was made by examining the sensitivity to gas adsorption for a few photon energies of typically less than 30 eV. A more stringent test would be to examine the binding energy over a wide photon energy range for the same $\mathbf{k}_{\parallel}$ (the component of the photoelectron wave vector parallel to the sample surface), where a surface state should show a constant binding energy. The present normal emission data confirm that some of the previously identified surface-state features are indeed dispersionless over a wide photon energy range. We have also examined the effect of hydrogen adsorption on Ge(111)-$c(2\times8)$.

It has been shown recently that cleave-induced surface disorder can be correlated with angle-resolved photoemission spectra.[20] Surface umklapp processes induced by surface reconstruction can generate extra spectral features in the photoemission spectra and cause difficulties in band mapping.[18] Near-surface strain associated with reconstruction can also cause broadening of the electron crystal momentum. In the latter two cases the atoms near the surface have an ordered (but not bulklike) arrangement; the different ordering is responsible for the effects observed.

Reconstruction-induced effects may be minimized if the surface reconstruction is suppressed. By saturating the Ge(111)-$c(2\times8)$ surface with hydrogen, the surface becomes (1×1). We hoped that the photoemission spec-

tra from Ge(111) could be significantly simplified by this technique to facilitate easy band mapping. But the resulting spectra after hydrogenation did not show significant changes. We will discuss the possible implications of this results with regard to near-surface strain of clean and hydrogenated Ge(111) surfaces.

This paper is organized as follows. We discuss the experimental details in Sec. II. In Sec. III, we present results and discussion. The dispersive and nondispersive spectral features of each of the systems studied are reviewed. The conclusions are given in Sec. IV.

II. EXPERIMENTAL

The photoemission measurements were performed at the Synchrotron Radiation Center of the University of Wisconsin—Madison. Synchrotron radiation from the 240-MeV storage ring Tantalus was dispersed by either a Seya monochromator or a 3-m toroidal grating monochromator (TGM). The photoemitted electrons in the sample-normal direction were analyzed with a hemispherical analyzer having an acceptance full angle of 3°. Spectra were taken for three different samples: Ge(111), Si(100), and Si(111). The overall energy resolutions for the three samples at different photon energies $h\nu$ were as follows: for Ge(111), about 0.2 eV at $h\nu=11$ eV, 0.3 eV at $h\nu=34$ eV, and 0.6 eV at $h\nu=70$ eV; for Si(100), about 0.2 eV at $h\nu=12$ eV, 0.3 eV at $h\nu=22$ eV, 0.4 eV at $h\nu=30$ eV, and 0.7 eV at $h\nu=98$ eV; and for Si(111), about 0.2 eV at $h\nu=12$ eV, 0.4 eV at $h\nu=30$ eV, and 0.5 eV at $h\nu=80$ eV. The energy position of the substrate Fermi level was determined by measuring the Fermi-level position of a gold foil in electrical contact with the substrate.

The p-Ge(111) sample was aligned by Laue diffraction to within 1°, mechanically polished to a mirror finish, and chemically etched with dilute NaOCl before insertion into the vacuum chamber. The $c(2\times8)$ surface was prepared by repeated sputtering and annealing until a sharp $c(2\times8)$ high-energy electron diffraction (HEED) pattern was observed. The surface cleanliness was checked with Auger-electron spectroscopy (AES). We adsorbed hydrogen on the clean $c(2\times8)$ surface by exposing it to 1200-langmuirs [1 langmuir (L)$=10^{-6}$ Torr sec] hydrogen gas in the presence of a hot (2000 °C) tungsten filament. Subsequent HEED measurements showed the surface pattern to be (1×1).

Both silicon samples came from commercially polished wafer stock. The n-Si(111) substrate was resistively heated to about 1250 °C to obtain a contamination-free (7×7) surface, as determined by *in situ* AES and HEED measurements. The p-Si(100) substrate was resistively flash-heated at about 900 °C a few times, until a sharp (2×1) HEED pattern [consisting of (2×1) domains in two orientations 90° apart and differing by an atomic step] appeared. This method of preparation has been found to produce a reproducibly smooth, chemically clean Si(100)-(2×1) surface.[21]

The base pressure of the vacuum chamber used during these measurements was about 1×10^{-10} Torr. Under these conditions, the sample surfaces would typically exhibit signs of contamination after several hours. During the actual measurements, either clean surfaces were regenerated or new samples were inserted more frequently than this.

The experimental geometries for the three samples were as follows. For the Ge and Si(111) surfaces, define a Cartesian coordinate system with the x axis parallel to the $[11\bar{2}]$ crystalline direction, $y\|[\bar{1}10]$, and $z\|[111]$ (the surface normal). Then the direction cosines of the incident photon wave vector for Si(111) were $(+0.57, 0, -0.82)$; for Ge(111) they were $(+0.71, 0, -0.71)$. In the case of Si(100), the Cartesian coordinate system is defined by the crystalline $\langle 100\rangle$ directions; the direction cosines

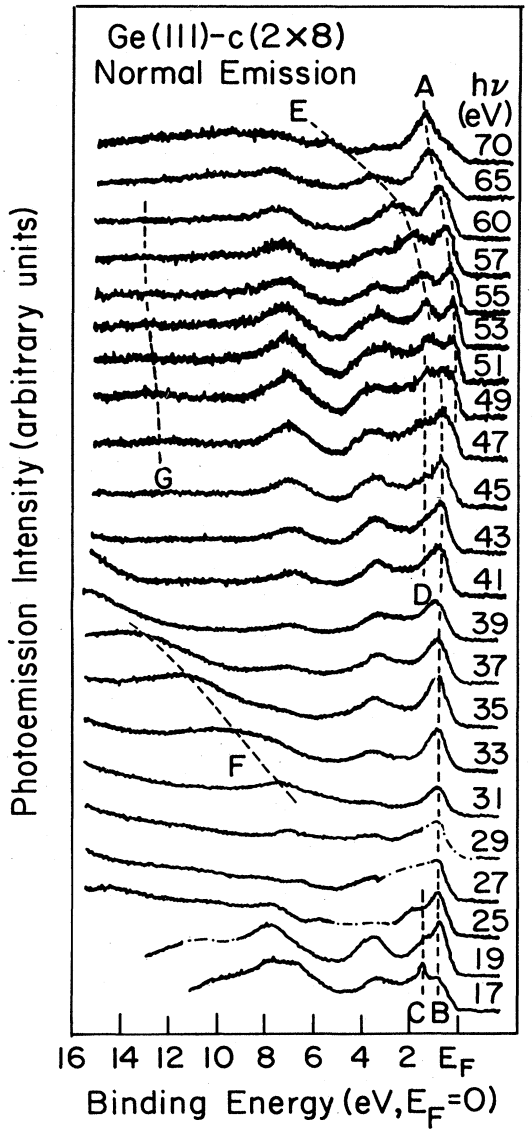

FIG. 1. Normal-emission spectra for Ge(111)-$c(2\times8)$ taken with the indicated photon energies. The binding energy scale is referred to the Fermi level at E_F. Several peaks are indicated by dashed curves and labeled A—G for clarity.

incident photon wave vector were (+0.57, 0, −0.82). The photon vector potential **A** lay in the plane defined by the x and z axes of all three samples studied.

III. RESULTS AND DISCUSSION

A. Ge(111)-$c(2\times8)$

Figure 1 shows a set of normal emission spectra of Ge(111)-$c(2\times8)$ obtained over a photon energy range of 17 to 70 eV. The binding energy scale is referred to the Fermi level E_F. There are many clearly identifiable emission features. The peak labeled G is relatively weak in the $h\nu > 51$-eV spectra and does not show up as clearly in the figure. Its presence is quite evident in much larger plots (not shown). Features labeled A—G will be discussed below, some of which are dispersive as a function of $h\nu$. Two broad features with binding energies of about 7 and 3.5 eV are also visible over most of the photon energies used; they are related to features in the density of states. They do not lead to very useful information about the band dispersions. Stray second-order diffraction in the TGM (operated in the first order) caused the appearance of the Ge-3d core level with reduced intensity in the $h\nu = 19$-,25-,27-, and 29-eV spectra. Portions of these spectra which are uncertain by this effect have been replaced by arbitrary dashed-dotted curves in Fig. 1.

1. Dispersive peaks and bulk valence-band dispersion

Peaks A, E, F, and G exhibit dispersive behavior. Peak F is derived from the Ge MVV Auger transition and has nearly constant kinetic energy. Peaks A, E, and G are derived from photoemission. The assignments of these peaks are facilitated by comparison of the present spectra with previous work done on related systems: GaAs(100), GaAs(110), and Ge(100).[11,12,17,18]

We have displayed in Fig. 2 the theoretical valence-band dispersions of Ge as solid curves along the Γ-Λ-L (or [111]) and the Γ-Δ-X (or [100]) directions, as calculated by Chelikowsky and Cohen.[16] Four different valence bands are labeled 1—4 in Fig. 2. Since bands 3 and 4 are nearly degenerate and cannot be resolved experimentally, we will refer to them as bands 3-4 in the following. The binding energy scale in Fig. 2 is referred to the valence-band maximum (VBM) at E_V. Previous $E_F - E_V$ measurements for Ge(111)-$c(2\times8)$ gave a value of about 0.1 eV.[22] We have used $E_F - E_V = 0.1$ eV in this analysis. The solid circles are data points from Ref. 12.

Referring to the discussion in Refs. 17 and 18, we have assigned peaks A, E, and G to direct transition peaks from bands 3-4, 2, and 1, respectively. We followed the technique discussed in Refs. 17 and 18 to map the band dispersions using the peak positions of A, E, and G; the uncertainties and the limitations of this technique have been discussed in detail in these references and will not be described here. The final-state band is approximated by a free-electron final-state band, assuming an inner potential of 7.8 eV referred to E_F, or 7.7 eV referred to the VBM.[12] The resulting dispersions are shown in Fig. 2 as open circles; we have also shown the estimated typical error. The theoretical and experimental results are in excellent agreement.

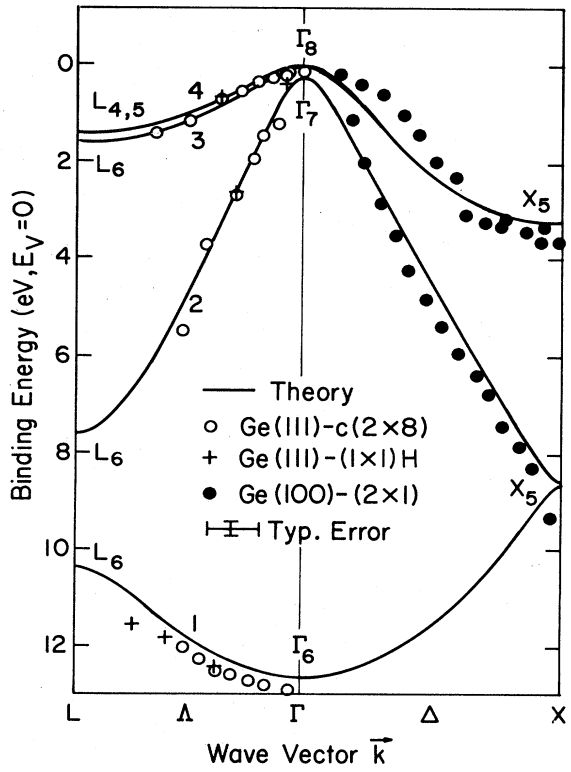

FIG. 2. Bulk valence-band dispersion relations of Ge. The solid curves are from theory. The binding energy scale is referred to the VBM at E_V. The open circles, crosses, and solid circles are data points obtained from Ge(111)-$c(2\times8)$, Ge(111)-(1×1)H, and Ge(001), respectively.

We also obtained bulk valence-band normal emission data from the hydrogenated Ge(111) surface, using $h\nu = 29$—60 eV. The spectra are shown in Fig. 3. A comparison of the binding energies of bulk transition features with the $c(2\times8)$ data in the regime of overlapping photon energies gave $E_F - E_V = 0.2$ eV for Ge(111)-(1×1)H. Apart from this small overall shift in band bending, the spectra for Ge(111)-H are very similar to those for Ge(111)-$c(2\times8)$ in terms of relative peak intensities and peak positions. We followed the same band-mapping procedure; the resulting experimental dispersions are shown as crosses in Fig. 2. The peak corresponding to band 1 shows up slightly more clearly in the case of Ge(111)-H, and therefore, we could extend the experimental dispersion curve of band 1 somewhat to the left in Fig. 2 beyond that determined from the data for Ge(111)-$c(2\times8)$.

2. Nondispersive peaks and surface states

Peaks B, C, and D are nondispersive in Fig. 1. C and D have identical binding energies of 1.4 eV relative to E_F; B is located 0.8 eV below E_F. Upon hydrogenation of the $c(2\times8)$ surface, features B and D remained unchanged in

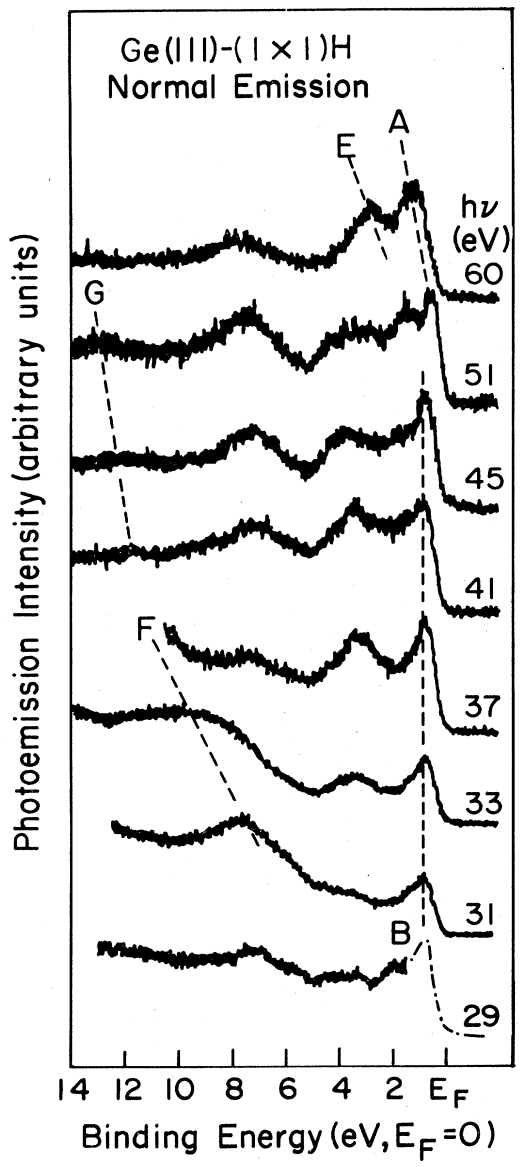

FIG. 3. Normal-emission spectra for Ge(111)-(1×1)H taken with the indicated photon energies. The binding energy scale is referred to the Fermi level at E_F. Several peaks are indicated by dashed curves and labeled the same way as in Fig. 1.

intensity over the range of overlapping photon energies ($h\nu$=29—60 eV) used to study Ge(111)-H and Ge(111)-$c(2\times8)$.

Bringans and Hochst[13] have studied Ge(111)-$c(2\times8)$ and Ge(111)-H with angle-resolved photoemission at $h\nu$=16.85 and 21.22 eV. Their Ge(111)-$c(2\times8)$ data are similar to ours when interpolated over the range of overlapping photon energies. These authors observed 0.8-eV and 1.4-eV binding-energy features (referred to E_F) in their normal emission spectra at both photon energies used. The two features nearly disappeared upon hydrogenation of the reconstructed surface. On the basis of this information, Bringans and Hochst assigned these features to surface-state emission.

Our results show that the feature at 0.8-eV binding energy (feature *B* in Fig. 1) is indeed dispersionless over a wide photon energy range, consistent with the surface-state assignment. However, this feature is insensitive to hydrogen adsorption in the photon energy range of 29—60 eV in our present data (see Fig. 3). Since there is not any bulk critical point with high density of states at this binding energy, this peak is not likely to be a bulk feature. It is possible, however, that hydrogenation of the Ge surface selectively attenuates the emission intensity of this feature over a limited range of photon energies (e.g., 16—22 eV). If so, this surface state cannot be sensitive to the $c(2\times8)$ long-range order. Peak *D* in Fig. 1 has a binding energy close to that of the $L_{4,5}$ or L_6 critical point. Whether this peak is derived from one of these bulk critical points or from the same surface state observed at lower photon energies (peak *C* in Fig. 1) cannot be determined unambiguously from the existing data. But it is definitely insensitive to hydrogen adsorption and the associated change in surface reconstruction.

Himpsel *et al.*,[3] using a photon energy of 22 eV and an angle-integrated geometry, also observed that these two surface states disappeared upon hydrogen adsorption. But the same two states were observed on a laser-annealed Ge(111)-(1×1) surface. However, this observation is not inconsistent with our present results because different photon energies were used. More detailed research is needed to clarify the nature of these surface states.

3. *Implications with regard to near-surface strain*

Hydrogenation of Ge(111)-$c(2\times8)$ changes the surface to (1×1). But the photoemission spectra remain essentially unchanged, although one might have expected possible simplification of the spectra. Like Si(111)-(7×7), Ge(111)-$c(2\times8)$ may have a surface strain field extending deep below the surface. The strain field is not necessarily removed by hydrogenation. For example, stacking faults near the surface [which may exist for Si(111)-(7×7)] (Refs. 23—27) might not be significantly affected by hydrogenation. The electron escape depth is typically about 5—10 Å in our measurements. If the strain field reaches about the same depth or more [speculated to be the case for Si(111)-(7×7)], the photoemission spectra will show large contributions from electronic states having significant amplitude within the strained lattice layer. The component of the electron wave vector in the surface normal direction becomes smeared out in the inhomogeneously strained region near the surface; therefore, photoemission, even angle-resolved, will primarily probe the density-of-state features in this region. The density of states in the strained layer generally consists of surface-state contributions (from dangling bonds, for example) and bulklike contributions which may be similar to the true bulk contribution but modified by strain. Emission from the true bulk will be weak if the strained region is thick. We speculate that Ge(111)-$c(2\times8)$ and Ge(111)-(1×1)H have similar surface strain fields extending into the bulk a distance comparable to the electron escape depth. This is why both surfaces exhibit very similar photoemission spectra over a wide photon energy range, which show sig-

nificant contributions from features other than dispersive bulk-derived direct transitions. By comparison, the normal emission spectra of cleaved GaAs(110)-(1×1),[17] for example, exhibit much more pronounced dispersive bulk-derived direct transition peaks. The strain field at the GaAs(110) surface probably has a shorter range. The Si(111)-(7×7) surface, to be discussed below, probably has an even more extensive strain field near the surface than Ge(111)-$c(2\times8)$.

B. Si(111)-(7×7)

Our data for the Si(111)-(7×7) surface are shown in Fig. 4. This set of normal-emission spectra was taken over $h\nu=12-78.9$ eV. The binding energy is referred to the Fermi level E_F. There are no clearly discernible dispersive spectral features in the data for $h\nu$ greater than 25 eV, which is the important range for band mapping. Therefore, we do not have experimental dispersion curves for Si from this data. Three nondispersive features, labeled *A*, *B*, and *C*, are visible over most of the range of photon energies used. The measured binding energies of *A*, *B*, and *C* are 0.3, 0.9, and 1.8 eV, respectively. Most authors agree that these three features are derived from surface-state emission.[2,4,5,14] We have found the 0.3-eV feature to be quite sensitive to surface quality; it becomes sharper and more intense for samples with lower background in the (7×7) HEED pattern. This may be pertinent to the earlier controversy over whether or not there is significant emission from near the Fermi edge.[4]

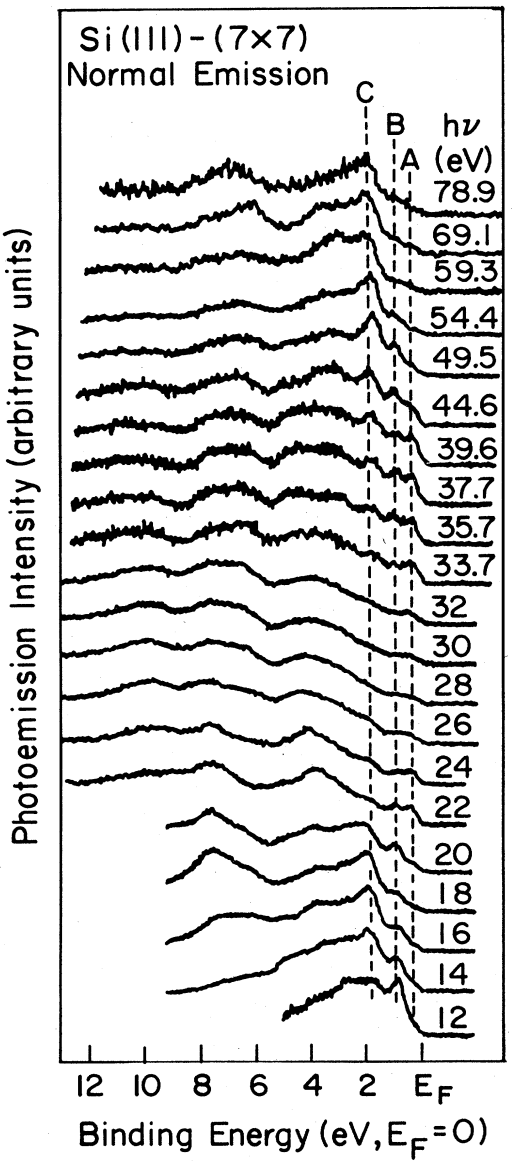

FIG. 4. Normal-emission spectra for Si(111)-(7×7) taken with the indicated photon energies. The binding energy scale is referred to the Fermi level at E_F. The three low-binding-energy peaks labeled *A*, *B*, and *C* are surface-state features.

The remaining portions of our Si(111)-(7×7) spectra consist largely of broad features at constant binding energies. Chelikowsky and Cohen's[16] Si band-structure calculation yields critical points at 9.5 eV (L_2) and 6.9 eV (L_1). After making allowance for $E_F-E_V=0.63$ eV,[28] we see that the two lowest broad features have about the same binding energies as those of the two critical points. Nevertheless, this association remains uncertain.

Our failure to observe bulk-derived direct transitions into a free-electron-like final band over a wide photon energy range probably indicates that the surface reconstruction-induced distortion of the bulk crystal extends to a fairly large depth at least on the order of the photoelectron escape depth minimum for Si, about 5 to 7 Å.[29] This is similar to (and perhaps to an even greater degree than) the situation for Ge(111)-$c(2\times8)$ and Ge(111)-(1×1)H already discussed above. On the other hand, Hansson and Flodstrom[5] have shown for Si(111)-(7×7) and $h\nu=7-11.6$ eV that bulklike transitions are observable in their normal-emission spectra. The photoelectron escape depth during their study would have been of order 20 Å.[29]

There is a long-standing controversy over the structure of the Si(111)-(7×7) surface. Although this surface has been imaged in real space with scanning tunneling microscopy,[30] interpretation of these findings remains an open question. Ion channeling and blocking data seem to indicate the existence of stacking faults near the surface.[25] But a recent modified adatom model was capable of explaining most experimental results satisfactorily without invoking stacking faults.[27] Most authors agree, however, that the surface strain probably extends several atomic layers deep. This may explain the lack of bulk dispersive direct transitions in our spectra.

C. Si(001)-(2×1)

Figure 5 shows a set of normal-emission spectra of Si(100)-(2×1) obtained over a photon energy range of 12 to 98.4 eV. The binding energy is referred to the Fermi level E_F. For clarity, some of the closely-spaced low-binding-energy features are connected by dashed lines and labeled *A*–*F* in Fig. 5. Two broad emission features at binding energies of 7 and 12 eV appear in most of the spectra. These broad features are related to the density of

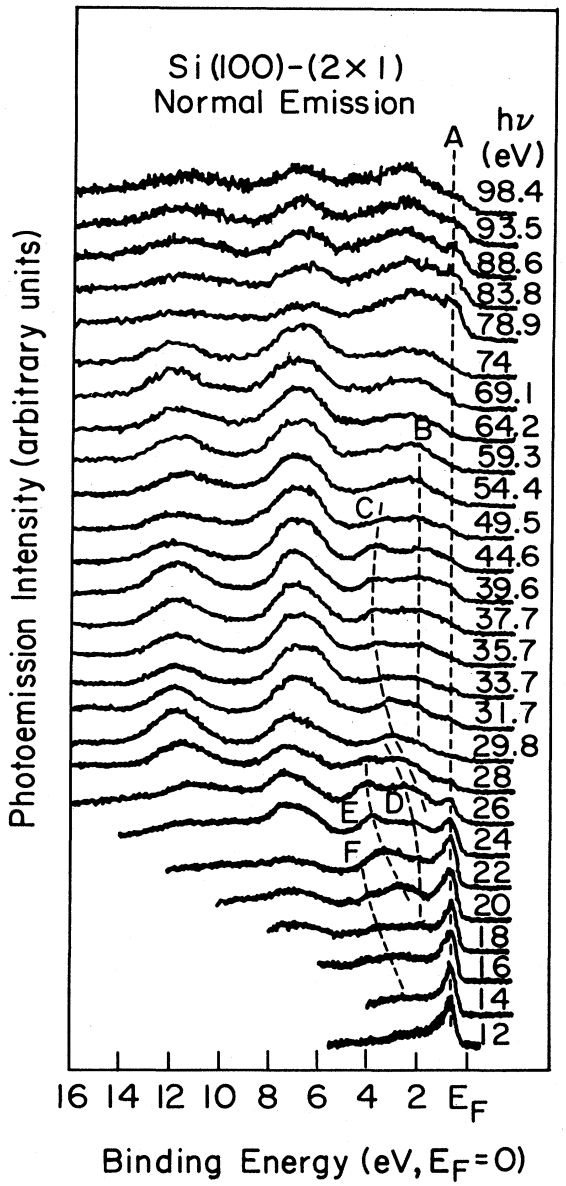

FIG. 5. Normal-emission spectra for Si(100)-(2×1) taken with the indicated photon energies. The binding energy scale is referred to the Fermi level at E_F. Several low-binding-energy features are indicated by dashed curves and labeled A—F for clarity.

states and do not provide very useful information about the band dispersion curves.

1. *Dispersive peaks and bulk valence-band dispersions*

Peaks C, D, E, and F clearly exhibit dispersive behavior. The assignments of these peaks are facilitated by comparison of the present spectra with previous work done on related systems. We have displayed in Fig. 6 the theoretical valence-band dispersions of Si along the two high-symmetry directions: Γ-Δ-X or the [001] direction, and Γ-Λ-L or the [111] direction. These dispersions were

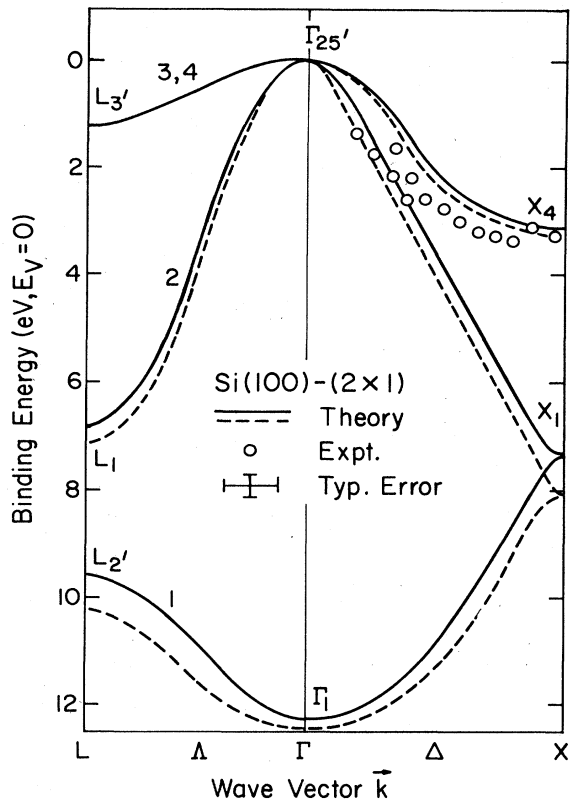

FIG. 6. Bulk valence-band dispersion relations of Si. The solid and dashed curves are theoretical results from a nonlocal and local pseudopotential calculation, respectively. The open circles are data points. The binding-energy scale is referred to the VBM at E_V.

obtained by Chelikowsky and Cohen[16] using a local pseudopotential (dashed curve) or a nonlocal pseudopotential (solid curve) technique. Four different valence bands are labeled in Fig. 6. The two uppermost bands, bands 3 and 4, are degenerate if the small spin-orbit interaction is ignored. All energies in the figure are referred to the VBM at E_V, which is 0.35 eV below E_F (Ref. 6) for Si(001)-(2×1).

We have assigned peaks C and D to direct transitions from bands 3-4 and 2, respectively, based upon the discussion of Refs. 17 and 18. We used an inner potential of 4.2 eV for the free-electron band referred to the Fermi level E_F. This value was obtained from a low-energy electron diffraction measurement of 9 eV for the inner potential (relative to the vacuum level)[31] and a Si(001)-(2×1) surface work function measurement of 4.85 eV.[6] Another value for the inner potential, 12.4 eV, was obtained in Refs. 8 and 19. These authors used lower kinetic-energy electrons (~5—17 eV) then Ref. 31 (40—180 eV). The inner potential depends upon the final-state electron kinetic energy, so there is no *a priori* reason to expect these results to be identical. Since the range of kinetic energies (~20—40 eV) in our data fell between those used in Refs. 8 and 19, and Ref. 31, we chose the inner potential value that gave the best agreement between theory and experi-

ment. The resulting experimental dispersions are shown in Fig. 6 as open circles; the estimated typical error is also shown.[17,18] The theory and experiment are within reasonable agreement.

Peaks E and F of Fig. 5 are also dispersive and therefore derived from bulk transitions. But their assignments cannot be certain without an accurate knowledge of the final-state band dispersions.[17,18] We will not discuss them further here.

2. *Nondispersive peaks and surface states*

Peaks A and B of Fig. 5 are nondispersive. Peak A, located 0.7 eV below E_F, has been observed and assigned to surface-state emission mainly on the basis of data taken with $h\nu$ less than 21.2 eV and its sensitivity to gas adsorption.[6] Our present spectra show that this peak is observable and dispersionless over a very wide photon energy range, confirming the surface-state assignment. Our spectra compare very well to the spectra of Ref. 6 when properly interpolated over the range of overlapping photon energies. Peak B, visible for $h\nu$ larger than 29.8 eV, has a binding energy of about 2 eV. This peak and a few other broad spectral features in Fig. 5 cannot be definitively assigned on the basis of the present data.

IV. SUMMARY AND CONCLUSION

We have performed angle-resolved photoemission measurements on Si(111)-(7×7), Si(100)-(2×1), Ge(111)-c(2×8), and Ge(111)-(1×1)H in a normal emission geometry over a wide range of photon energies. From our studies of Ge(111)-c(2×8), we determined experimental bulk valence-band dispersion relations from the Γ point to the L point in the Brillouin zone along the [111] direction of Ge. In this case, theory and experiment are in excellent agreement. Some data was also collected from the hydrogenated Ge(111) surface, whose spectra were nearly identical to those of Ge(111)-c(2×8) in terms of relative peak positions and intensities. Two features in the Ge(111)-c(2×8) and Ge(111)-H spectra with constant binding energies of 0.8 and 1.4 eV (referred to E_F) were observed over a wide photon energy range. They are likely to be derived from surface-state emission.

The Si(111)-(7×7) data have three surface-state emission features with binding energies of 0.3, 0.9, and 1.8 eV (referred to E_F). They are visible over most of the photon energies used. No bulk direct transitions to a free-electron-like final band were clearly identifiable in these spectra. Apart from the surface states, most spectra consist of a few broad features with constant binding energies whose intensities vary slowly as a function of the photon energy. This behavior is quite different from that of GaAs(110) whose spectra are dominated by bulk-derived direct transition peaks to a free-electron-like final band. This qualitative difference may be due to a more extended strain field near the surface in Si(111)-(7×7) than in GaAs(110) smearing the electron crystal momentum and modifying the electronic states.

From our studies of Si(100)-(2×1), we determined E-versus-k dispersion relations from the Γ point to the X point in the Brillouin zone along the [100] direction for the uppermost valence bands of Si. The experimental band dispersions are in reasonable agreement with the theoretical calculations of Chelikowsky and Cohen. We have observed the 0.7-eV binding energy (referred to E_F) Si(100)-(2×1) surface state up to the highest photon energy (98.4 eV) used in the present experiment.

ACKNOWLEDGMENTS

This material is based upon work supported by the Department of Energy, Division of Materials Sciences, under Contract No. DE-AC02-76ER01198. Some of the equipment used for this research was obtained with grants from the National Science Foundation (Grant No. DCR-8352083), the IBM Research Center (Faculty Development Award), the Research Corporation, and the General Motors Research Laboratories. We are grateful to the staff of the Synchrotron Radiation Center of the University of Wisconsin for assistance. The Synchrotron Radiation Center is supported by the National Science Foundation under Contract No. DMR-8020164. We acknowledge the use of central facilities of the Materials Research Laboratory of the University of Illinois which are supported by the Department of Energy and the National Science Foundation.

[1]D. E. Eastman, J. Vac. Sci. Technol. **17**, 492 (1980).
[2]F. J. Himpsel, Physica **117&118B**, 767 (1983).
[3]F. J. Himpsel, D. E. Eastman, P. Heimann, B. Reihl, C. W. White, and D. M. Zehner, Phys. Rev. B **24**, 1120 (1981).
[4]F. Houzay, G. M. Guichar, R. Pinchaux, P. Thiry, Y. Petroff, and D. Dagneaux, Surf. Sci. **99**, 28 (1980).
[5]H. Neddermyer, U. Misse, and P. Rupieper, Surf. Sci. **117**, 405 (1982); G. V. Hansson and S. A. Flodstrom, J. Vac. Sci. Technol. **16**, 1287 (1979).
[6]R. I. G. Uhrberg, G. V. Hansson, J. M. Nicholls, and S. A. Flodstrom, Phys. Rev. B **24**, 4684 (1981); F. J. Himpsel and D. E. Eastman, J. Vac. Sci. Technol. **16**, 1297 (1979).
[7]F. J. Himpsel, P. Heimann and D. E. Eastman, Phys. Rev. B **24**, 2003 (1981); R. I. G. Uhrberg, G. V. Hansson, J. M. Nicholls, and S. A. Flodstrom, Surf. Sci. **117**, 394 (1982).
[8]R. I. G. Uhrberg, G. V. Hansson, U. O. Karlsson, J. M. Nicholls, P. E. S. Persson, S. A. Flodstron, R. Engelhardt, and E.-E. Koch, Phys. Rev. Lett. **52**, 2265 (1984).
[9]F. Solal, G. Jezequel, A. Barski, P. Steiner, R. Pinchaux, and Y. Petroff, Phys. Rev. Lett. **52**, 360 (1984).
[10]J. M. Nicholls, G. V. Hansson, U. O. Karlsson, R. I. G. Uhrberg, R. Engelhardt, K. Seki, S. A. Flodstrom, and E.-E. Koch, Phys. Rev. Lett. **52**, 1555 (1984).
[11]J. G. Nelson, W. J. Gignac, R. S. Williams, S. W. Robey, J. G. Tobin, and D. A. Shirley, Phys. Rev. B **27**, 3924 (1983); Surf. Sci. **131**, 290 (1983).
[12]T. C. Hsieh, T. Miller, and T.-C. Chiang, Phys. Rev. B **30**, 7005 (1985).
[13]R. D. Bringans and H. Hochst, Phys. Rev. B **25**, 1081 (1982).
[14]J. E. Demuth, B. N. J. Persson, and A. J. Schell-Sorokin,

Phys. Rev. Lett. **51**, 2214 (1983).
[15]See, for example, J. C. Phillips, in *Solid State Physics,* edited by H. Ehrenreich, F. Seitz, and D. Turnbull (Academic, New York, 1966), Vol. 18, p. 56.
[16]J. R. Chelikowsky and M. L. Cohen, Phys. Rev. B **14**, 556 (1976).
[17]T.-C. Chiang, J. A. Knapp, M. Aono, and D. E. Eastman, Phys. Rev. B **21**, 3513 (1980); T.-C. Chiang, J. A. Knapp, D. E. Eastman, and M. Aono, Solid State Commun. **31**, 917 (1979).
[18]T.-C. Chiang, R. Ludeke, M. Aono, G. Landgren, F. J. Himpsel, and D. E. Eastman, Phys. Rev. B **27**, 4770 (1983).
[19]D. Straub, L. Ley, and F. J. Himpsel, Phys. Rev. Lett. **54**, 142 (1985).
[20]F. Cerrina, J. R. Myron, and G. J. Lapeyre, Phys. Rev. B **29**, 1798 (1984).
[21]M. Hanbucken, H. Neddermeyer, and J. A. Venables, Surf. Sci. **137**, L92 (1984).
[22]M. Buchel and H. Luth, Surf. Sci. **50**, 451 (1975); G. M. Guichar, G. A. Garry, and C. A. Sebenne, Surf. Sci. **85**, 326 (1979).
[23]E. G. McRae, Phys. Rev. B **28**, 2305 (1983).
[24]F. J. Himpsel, Phys. Rev. B **27**, 7782 (1983).
[25]P. A. Bennett, L. C. Feldman, Y. Kuk, E. G. McRae, and J. E. Rowe, Phys. Rev. B **28**, 3656 (1983).
[26]R. M. Tromp and E. J. Van Loenen, Phys. Rev. B **30**, 7352 (1984).
[27]D. J. Chadi, Phys. Rev. B **30**, 4470 (1984).
[28]F. J. Himpsel, G. Hollinger, and R. A. Pollak, Phys. Rev. B **28**, 7014 (1983).
[29]H. Gant and W. Monch, Surf. Sci. **105**, 217 (1981).
[30]G. Binnig, H. Rohrer, C. H. Gerber, and E. Weibel, Phys. Rev. Lett. **50**, 120 (1983).
[31]W. S. Yang, F. Jona, and P. M. Marcus, Phys. Rev. B **28**, 2049 (1983).